

## Letters

### Experimental Verification of an Exact Evanescent Light Scattering Model for TIRM

Christopher Hertlein,<sup>\*,†</sup> Norbert Riefler,<sup>‡</sup> Elena Eremina,<sup>‡</sup> Thomas Wriedt,<sup>‡</sup> Yuri Eremin,<sup>§</sup>  
Laurent Helden,<sup>\*,†</sup> and Clemens Bechinger<sup>†</sup>

2. Physikalisches Institut, Universität Stuttgart, Pfaffenwaldring 57, 70569 Stuttgart, Germany,  
Verfahrenstechnik, Universität Bremen, 28334 Bremen, Germany, and Faculty of Applied Mathematics and  
Computer Science, Moscow State University, Lenin's Hills, 119992 Moscow, Russia

Received October 24, 2007. In Final Form: November 13, 2007

Total internal reflection microscopy (TIRM) is a method for the precise measurement of interaction potentials between a spherical colloidal particle and a wall. The method is based on single-particle evanescent wave light scattering. The well-established model used to interpret TIRM data is based on an exponential relation between scattering intensity and particle wall distance. However, applying this model for a certain range of experimental parameters leads to significant distortions of the measured potentials. Using a TIRM setup based on a two-wavelength illumination technique, we were able to directly measure the intensity distance relation revealing deviations from an exponential decay. The intensity–distance relations could be compared to scattering simulations taking into account exact experimental parameters and multiple reflections between a particle and the wall. Converging simulation results were independently obtained by the T-matrix method and the discrete sources method (DSM) and show excellent agreement with experiments. Using the new scattering model for data evaluation, we could reconstruct the correct potential shape for distorted interaction potentials as we demonstrate. The comparison of simulations to experiment intrinsically yields a new method to determine absolute particle–wall distances, a highly desired quantity in TIRM experiments.

#### Introduction

Total internal reflection microscopy (TIRM)<sup>1,2</sup> is a highly sensitive method of determining particle–wall interactions with a force resolution in the 10 fN range. It has been successfully applied to measure various types of interactions such as depletion forces and electrostatic and magnetic interactions.<sup>3–8</sup> The basic

principle in TIRM is to measure interaction potentials between a substrate and a colloidal particle suspended in a liquid. This is achieved by creating an evanescent field via the total internal reflection of an incident laser beam at the substrate–liquid interface. For total internal reflection, the illumination has to be at an angle that is larger than the critical angle given by the refractive indices of the substrate and liquid. The intensity of the evanescent field decays exponentially into the solvent. A particle undergoing Brownian motion in the liquid close to the interface scatters light out of the evanescent field with an intensity depending on the particle–wall distance  $z$ . For a TIRM measurement, the intensity  $I$  of the scattered light is typically

\* Corresponding authors. E-mail: c.hertlein@physik.uni-stuttgart.de;  
l.helden@physik.uni-stuttgart.de.

† Universität Stuttgart.

‡ Universität Bremen.

§ Moscow State University.

(1) Walz, J. *Curr. Opin. Colloid Interface Sci.* **1997**, *2*, 600–606.

(2) Prieve, D. *Adv. Colloid Interface Sci.* **1999**, *82*, 93–125.

(3) Helden, L.; Roth, R.; Koenderink, G.; Leiderer, P.; Bechinger, C. *Phys. Rev. Lett.* **2003**, *90*, 048301.

(4) Helden, L.; Koenderink, G.; Leiderer, P.; Bechinger, C. *Langmuir* **2004**, *20*, 5662.

(5) Bevan, M.; Scales, P. *Langmuir* **2002**, *18*, 1474.

(6) Kleshchanok, D.; Tuinier, R.; Lang, P. R. *Langmuir* **2006**, *22*, 9121–9128.

(7) Blicke, V.; Babic, D.; Bechinger, C. *Appl. Phys. Lett.* **2005**, *87*, 101102.

(8) Blicke, V.; Speck, T.; Helden, L.; Seifert, U.; Bechinger, C. *Phys. Rev. Lett.* **2006**, *96*, 070603.

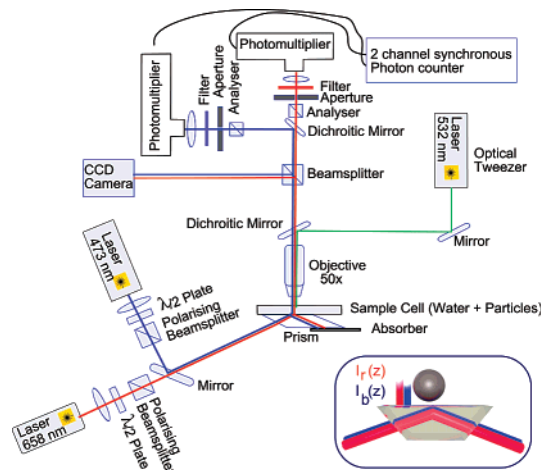


**Figure 1.** Schematic drawing of the setup. Two evanescent fields are created by separate lasers differing in their wavelengths. The inset shows the basic mechanism of the two-wavelength TIRM experiment.

recorded for 15 min. By creating a histogram of the measured intensities, one obtains probabilities  $p(I)$  that can be transformed into probabilities  $p(z)$ . This transformation depends crucially on the intensity–distance relation  $I(z)$ . At thermal equilibrium, the probabilities  $p(z)$  can be related to the particle–wall interaction potential  $\phi(z)$  by the Boltzmann factor  $p(z) = \exp(-\phi(z)/k_B T)$ , where  $k_B T$  is the thermal energy. The standard evaluation of TIRM data involves applying a purely exponential  $I(z) = I_0 \exp(-\xi z)$  relation where  $\xi^{-1}$  is the same decay constant as the penetration depth of the evanescent field intensity depending on the angle of incidence.<sup>9,10</sup> However, we recently demonstrated that because of multiple reflections between a particle and the wall such an exponential intensity–distance relation does not hold for certain experimental parameters such as a large penetration depth, a small particle–wall distance, and s-polarized illumination.<sup>11</sup> In these cases, exact simulation results show systematic deviations from exponential behavior appearing as oscillations in intensity–distance relations. Experimentally, these parameters yield interaction potentials displaying distortions of oscillatory shape if evaluated using an exponential  $I(z)$  dependence. Deviations from exponential behavior have also been observed by McKee et al. for small particle–substrate distances.<sup>12</sup> Using a new two-wavelength technique with TIRM, we experimentally verified the simulated intensity–distance relation calculated with two independent simulation methods—the T-matrix method and the discrete sources method (DSM)—under the above-mentioned conditions. The technique requires the use of two separate illuminating lasers, with each of them creating an independent evanescent field of which one is used as a reference under safe parameters. Combining this technique with the new model, measured interaction potentials can be corrected with respect to distortions, enabling TIRM measurements over a wider range of experimental parameters.

### Experiment

In Figure 1, a schematic drawing of the experimental setup is shown. Two laser beams with wavelengths of  $\lambda_r = 658$  nm (red) and

$\lambda_b = 473$  nm (blue) were coupled in the sample cell via a glass prism under the same angle  $\theta > \theta_c$  that is larger than the critical angle. The evanescent field was generated at the glass–water interface. For refractive indices of water  $n_{\text{water}} = 1.333$  and glass  $n_{\text{glass}} = 1.515$ , the critical angle was  $\theta_c = 61.63^\circ$ . The deviation from the critical angle  $\theta_c$  could be varied for both lasers simultaneously. The penetration depths  $\xi^{-1}$  of the resulting evanescent field intensities were thus dependent only on the illumination wavelengths  $\lambda = \lambda_r$  and  $\lambda_b$  and were larger for  $\lambda_r$ .

$$\xi^{-1} = \frac{\lambda}{4\pi n_1 \sqrt{\sin^2 \theta - \sin^2 \theta_c}} \quad (1)$$

Here,  $n_1$  is the refractive index of the substrate, and  $\lambda$  is the wavelength of the incident light in vacuum. For illumination and detection, the polarization (p or s) of the laser light could be adjusted by means of a  $\lambda/2$  plate combined with a polarizing beamsplitter as the polarizer and another polarizing beamsplitter as the analyzer. The polarization has been adjusted for both lasers separately. To prevent lateral drift of the probe particle, optical tweezers with a wavelength of 532 nm were applied from above.<sup>13</sup> A 50 $\times$  microscope objective with a numerical aperture of 0.5 was used to observe the particle and to collect its scattering intensity. The particle was observed using a CCD camera, and the scattered light intensity was recorded using two photomultiplier tubes (PMT) (Hamamatsu R928p) suited for single-photon counting, allowing high detection efficiency and low noise. The output of the PMTs was recorded using an internally timed photon counter (Stanford Research Systems, SR400) yielding synchronized detection and connected to a PC for data collection. An interference filter was placed in front of each PMT, ensuring wavelength-sensitive detection without cross talk between the detectors.

All measurements were performed using colloidal particles suspended in water. The Debye screening length of the suspension was varied by adding NaCl to the circuit connected to the sample cell, and the concentration was monitored using a conductometer (COND 720 Innolab). As particles, we used polystyrene (PS 1.36  $\mu\text{m}$  from Duke Scientific, cat. no. 4013A, lot no. 28174; PS 3  $\mu\text{m}$  from Duke Scientific, lot no. 23774, cat. no. 4203A) and melamine beads (1.31  $\mu\text{m}$  from Microparticles, batch MF-COOH-S1343).

### Simulations

The simulation methods used to calculate intensity–distance relations exactly as applied in this work (the T-matrix method and the discrete sources method (DSM)) are described elsewhere in full detail and have already been introduced in connection with exact computations of intensity–distance relations for TIRM.<sup>11,14–16</sup> The methods are based on exact solutions of the electromagnetic problem of the TIRM geometry. They differ in the method of numerical calculation.

In the T-matrix method, all fields are expanded into spherical vector wave functions. The coefficients of the scattered field are computed using surface integrals. In the discrete sources method, all fields are expanded into a set of fictitious sources, and the coefficients are computed using a generalized point-matching scheme. To compute the scattering interaction between the particle and the plane surface in the T-matrix method, a representation of the fields as integrals over plane waves was used, whereas in DSM, Sommerfeld integrals are used to represent the Greens function of the half space.

(9) Suresh, L.; Walz, J.; Hirleman, E. Detection of Particles on Surfaces Using Evanescent Wave Scattering. In *Particles on Surfaces 5 and 6*; Mittal, K. L., Ed.; VSP: Utrecht, The Netherlands, 1999; pp 19–34.

(10) Prieve, D.; Walz, J. *Appl. Opt.* **1993**, *32*, 1629–1641.

(11) Helden, L.; Eremina, E.; Riefler, N.; Hertlein, C.; Bechinger, C.; Eremin, Y.; Wriedt, T. *Appl. Opt.* **2006**, *45*, 7299–7308.

(12) McKee, C. T.; Clark, S. C.; Walz, J. Y.; Ducker, W. A. *Langmuir* **2005**, *21*, 5783–5789.

(13) Walz, J. Y.; Prieve, D. C. *Langmuir* **1992**, *8*, 3073–3082.

(14) Wriedt, T.; Doicu, A. *Opt. Commun.* **1998**, *152*, 376–384.

(15) Eremin, Y.; Wriedt, T. *J. Quant. Spectrosc. Radiat. Transfer* **2004**, *89*, 53–65.

(16) Riefler, N.; Eremina, E.; Hertlein, C.; Helden, L.; Eremin, Y.; Wriedt, T.; Bechinger, C. *J. Quant. Spectrosc. Radiat. Transfer* **2007**, *106*, 464–474.

For the experimental results presented here, the agreement between the two independent simulation methods provided an internal check of the consistency and convergence of both methods.

### Data Evaluation and Results

To verify the simulated intensity–distance relations  $I(z)$  experimentally, one needs to extract this information from experimental data. This was achieved by applying a new two-color TIRM technique. This technique involves using one laser as a reference to calculate from it the particle–wall distance. This laser is set to parameters where the exponential  $I(z)$  is applicable.<sup>11</sup> The validity of the exponential model can be easily checked by obtaining interaction potentials in agreement with theoretical predictions (e.g. DLVO theory) and independent of (smaller) changes in penetration depth. In general, these parameters will apply to p polarization and a smaller penetration depth; therefore, the  $\lambda_b = 473$  nm laser is chosen as the reference providing information on the particle–substrate distance. The other one ( $\lambda_r = 658$  nm) is set to parameters where  $I(z)$  should be tested. Typically, these will be a larger penetration depth and s polarization because deviations from the exponential model are expected in this regime.<sup>11</sup> The synchronous measurement of both scattering lasers yields  $I_r(t)$  and  $I_b(t)$  where  $I_r$  and  $I_b$  are the intensities of wavelengths  $\lambda_r$  and  $\lambda_b$ , respectively. For the reference laser with  $\lambda_b = 473$  nm, one can invert the  $I_b(z_b)$  relation

$$I_b(z_b) = I_{b,0} f_b(z_b) = I_{b,0} \exp(-\xi_b z_b) \quad (2)$$

$$\Leftrightarrow z_b = \xi_b^{-1} \ln(I_b) + \underbrace{\xi_b^{-1} \ln(I_{b,0})}_{z_0} \quad (3)$$

The functional dependence  $f_b(z_b)$  of  $I_b(z_b)$  is an exponential with  $\xi_b^{-1}$  being the penetration depth of the evanescent field created by  $\lambda_b = 473$  nm. For simultaneous measurements  $z_r = z_b$ , the intensity of the  $\lambda_r = 658$  nm laser can be written as

$$I_r(z_r) = I_{r,0} f_r(z_r) \stackrel{z_r=z_b}{\Leftrightarrow} I_{r,0} f_r(z_b) \quad (4)$$

Here,  $f_r(z_b)$  is the distance dependence of the intensity for the  $\lambda_r = 658$  nm laser, which is not necessarily exponential and has to be compared to simulation results. The only free parameters are  $z_0$  and  $I_{r,0}$ . For the  $\lambda_r = 658$  nm laser  $I_{r,0}$  is a proportionality factor. The distance offset  $z_0$  is connected to the intensity of the  $\lambda_b = 473$  nm laser. (i.e.,  $I_{b,0}$ , see eq 3). Deviations are expected to manifest themselves in a non-exponential  $f_r(z_b)$  compared to an exponential  $f_b(z_b)$ .

### Polystyrene 1.36 $\mu\text{m}$

By applying the procedure described above, one can compare the results from the two consistent simulation methods with experimental data for different penetration depths. Figure 2 shows the results for a polystyrene particle with a diameter of 1.36  $\mu\text{m}$  in a 250  $\mu\text{M}$  NaCl solution and penetration depths of  $\xi_r^{-1}$  of 500, 300, and 151 nm for  $\lambda_r$  (corresponding to  $\xi_b^{-1} = 359, 216,$  and 109 nm for  $\lambda_b$ ). Results span a range of about 1.5  $\mu\text{m}$  in separation distance. For a direct comparison of experiment and simulation results, experimental data have been shifted along the  $z$  axis by  $z_0$  and rescaled as mentioned above with  $I_{r,0}$ .  $z_0$  and  $I_{r,0}$  are chosen by varying both values until the best overlap between simulations and experiment is achieved. The oscillations of the  $I(z)$  relations are a strong criterion for choosing the correct values. The deviations from exponential behavior are obvious, especially for the larger penetration depths in both experiment and simulations. In fact, these deviations are especially useful for determining the

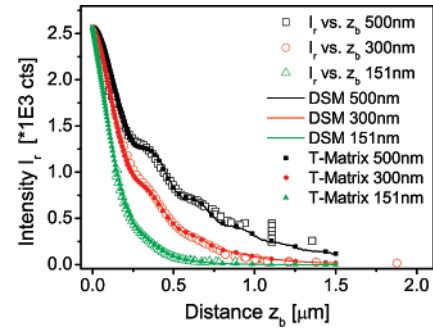


**Figure 2.** Intensity–distance curves for different penetration depths for a PS 1.36  $\mu\text{m}$  particle in a 250  $\mu\text{M}$  NaCl solution determined by plotting  $I_r$  versus  $z_b$  (open symbols). In addition, simulation results for the discrete sources (lines) and the T-matrix (closed symbols) methods are displayed.

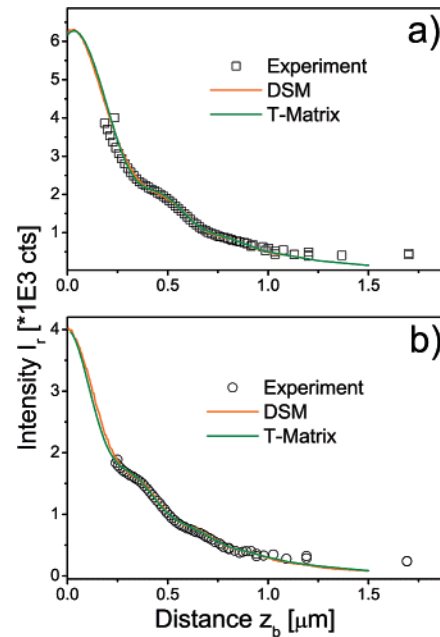


**Figure 3.** Intensity–distance curves at penetration depths of  $\xi_r^{-1} = 400$  nm ( $\lambda_r$ ) and  $\xi_b^{-1} = 287.5$  nm ( $\lambda_b$ ) determined by plotting  $I_r$  vs  $z_b$  for (a) a PS 3  $\mu\text{m}$  particle in a 100  $\mu\text{M}$  NaCl solution and (b) a melamine 1.3  $\mu\text{m}$  particle in a 250  $\mu\text{M}$  NaCl solution.

correct value for  $z_0$  and thereby allow the determination of absolute particle–wall distances. With a featureless exponential curve, this would not be possible. For the smallest penetration depths, almost no distortions could be identified, and  $I(z)$  is in agreement with the exponential model even for s-polarized illumination. The experimental results are in excellent agreement with the simulation results of both the T-matrix and DSM methods.

### Polystyrene 3 $\mu\text{m}$

To further verify the ability of the simulation method to give accurate predictions of  $I(z)$ , we have varied the particle size while keeping the refractive index constant.

For polystyrene beads with a diameter of 3  $\mu\text{m}$ , we applied the same evaluation as described above, and again there is an excellent agreement between experiment and T-matrix as well as DSM. In Figure 3a, the  $I(z)$  relation for a PS 3  $\mu\text{m}$  bead is shown at a 100  $\mu\text{M}$  NaCl concentration. The  $\lambda_r = 658$  nm laser was s polarized with a penetration depth of  $\xi_r^{-1} = 400$  nm whereas the  $\lambda_b = 473$  nm laser was p polarized with a corresponding penetration depth of  $\xi_b^{-1} = 287.5$  nm.

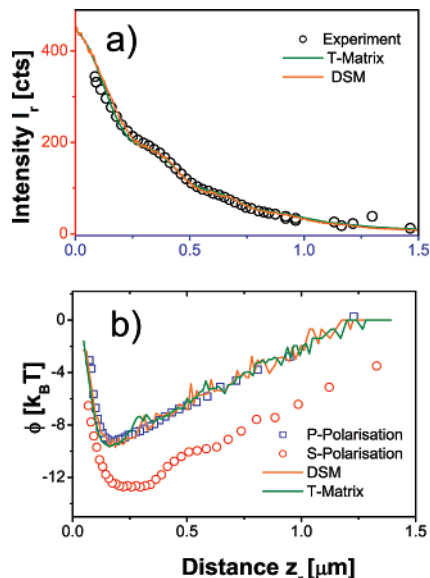


**Figure 4.** PS 1.36  $\mu\text{m}$  particle at  $\xi_r^{-1} = 400$  nm penetration depth and with 250  $\mu\text{M}$  NaCl concentration under s-polarized illumination and detection. (a) Intensity–distance relations obtained experimentally and via both simulation methods. (b) By applying the simulation results to obtain distances corresponding to intensity values of  $\lambda_r$ , one obtains the corrected potentials. For comparison, the potential before correction is displayed as open circles ( $\xi_b^{-1} = 287.5$  nm) under p polarization.

### Melamine 1.3 $\mu\text{m}$

To test the new scattering model for another parameter, we evaluated measurements for melamine particles with a similar diameter to that of PS 1.36  $\mu\text{m}$  in Figure 2 but with a different refractive index  $n_{\text{Mel}} = 1.68$  and compared them to the calculation results obtained for both methods. For a melamine particle with a diameter of 1.3  $\mu\text{m}$  in a 250  $\mu\text{M}$  NaCl solution, the results for  $I(z)$  are displayed in Figure 3b. Experimental data was obtained by simultaneously illuminating with a  $\lambda_r = 658$  nm laser (penetration depth  $\xi_r^{-1} = 400$  nm and s polarization) and a  $\lambda_b = 473$  nm laser (penetration depth  $\xi_b^{-1} = 287.5$  nm and p polarization). By varying the refractive index, the results of experiment and simulations agree well.

### Correcting Potentials

After the simulation results are experimentally verified, one can apply the simulated  $I(z)$  relation to evaluate the experimental data correctly. We compare for a PS 1.36  $\mu\text{m}$  particle the evaluation of interaction potentials obtained with simulated and simple exponential  $I(z)$  relations under s-polarized illumination with a large penetration depth of  $\xi_r^{-1} = 400$  nm for  $\lambda_r = 658$  nm. Figure 4a shows the  $I(z)$  relation displaying deviations from exponential decay. The open circles in Figure 4b show a potential

obtained by evaluating data of  $\lambda_r = 658$  nm “falsely” under the assumption of an exponential  $I(z)$ . The open squares in Figure 4b show the correct potential obtained by evaluating data from  $\lambda_b$ , the reference wavelength, with parameters where an exponential  $I(z)$  is appropriate (p polarization,  $\xi_b^{-1} = 287.5$  nm). Using the  $I(z)$  relation obtained by simulations, a  $z$  value can be assigned to each measured intensity of  $\lambda_r$ , and the interaction potential can be correctly calculated from a histogram of particle–wall distances. As a result, one obtains the new interaction potential for both simulation methods separately (solid lines). Thereby, remarkable agreement between the “correct” potential (squares) and the “corrected” potential (lines) is achieved. The distortions in the interaction potential have been removed upon applying the correct  $I(z)$  relation.

### Conclusions

We have extended the TIRM method with simultaneous two-wavelength illumination and detection. This allows us to test and verify calculated intensity–distance relations for TIRM measurements for different experimental conditions. Our experimental results agree perfectly with simulation results from DSM as well as the T-matrix method. By using the results for the intensity–distance relation, correct interaction potentials could be obtained even for extreme parameters where the simple exponential model would fail. Thus, we have demonstrated that T-matrix and DSM simulations are a powerful tool for the detailed analysis of evanescent light scattering data. This might pave the way for TIRM measurements with surfaces of high reflectivity or at larger penetration depths where deviations from the exponential scattering model due to multiple reflections between a particle and the wall become increasingly important. In addition, the comparison of simulated and measured  $I(z)$  relations intrinsically yields an extremely sensitive check of the correct value of  $z_0$ , the absolute particle–wall distance. Experimentalists using TIRM should be aware of the high sensitivity of  $I(z)$  relation and the derived interaction potentials with respect to the polarization and penetration depth of the evanescent field. P-polarized illumination is to be preferred, but as demonstrated, s-polarized illumination, even with a large penetration depth, can be understood and handled adequately, yielding correct interaction potentials. The simulation results enable a systematic study of  $I(z)$  relations with varying different experimental parameters. This will lead to predictions for the applicability range of the exponential model.

**Acknowledgment.** We thankfully acknowledge the financial support by the German Research Foundation (DFG) and we thank Uwe Rau and Denis Kobasevic for the sophisticated mechanical and electrical solutions needed to build the new  $2\lambda$  TIRM setup.

LA703322D